Investigation of the Integrity of aC:H Coatings on Stainless Steel Micro-Moulds during Thermal Cycling

C.A. Griffiths[a,*], A. Rees[a], G. Llewelyn[a] and O. V. Fonseca[b]

[a]*College of Engineering, Swansea University, Swansea SA1 8EN, UK*

[b]*School of Mechanical, Aerospace and Civil Engineering, University of Manchester, Sackville Street, Manchester M13 9PL, UK*

Abstract: Micro-injection moulding (µIM) is a key technology for scaling down larger geometry components and can include functional features at the micrometre scale and as far as the sub-micrometre length scale. Thermal cycling of amorphous hydrogenated carbon (aC:H) coated Stainless Steel (SS) has been investigated to simulate long-term micro-injection moulding (µIM) wearing and damage. Micro indentations and cracks were made into the mould and predictions of the crack behaviour were made using thermal expansion models. Validation of the results was performed with multiple heating and cooling cycles along with hardness measurements of the damage to the coating. The undamaged surfaces showed no major deformation but the cracks were shown to propagate and change in behaviour. The first two heat cycles of the testing had the most significant effect on the substrate with varying thermal expansions of materials being the main cause. The aC:H is shown to have excellent properties for mould tool applications but delamination could occur in areas susceptible to damaged and periodic surface inspection will be required preserve tool life.

1. INTRODUCTION

Micro-scale parts and the materials used for the moulds at these scales have increased in research importance as a result of the advanced developments in micro-engineering [1]. Micro-scale polymer objects can be mass produced with the use of microinjection moulding (µIM) at great ease due to the technological advances in this engineering sector from high demand in a wide application on the market, such as medical [2]. One of the main difficulties faced with µIM polymers: is the mould properties because at this level; the forces exerted on the polymer by demoulding are sufficient to cause permanent deformation [3]. Masato *et al.* [4] investigated the impact of the micromilling strategy on the reduction of the ejection force in µIM. Lower surface roughness was achieved by improving the milling parameters. Improving the micromilling strategy resulted in a reduction in surface roughness by 62%. They found that the effect of IM process parameters was considerably smaller compared to that of mould surface finish. They also found that by increasing the packing pressure, ejection stress was increased due to the higher replication and therefore higher mechanical bounding at the part to mould interface.

However, a coating with a lower level of surface friction than typical metals used for moulds, such as steel, can be added to the mould to decrease the ejection stress [5]. Griffiths *et al*. [6] report how to monitor such forces during ejection of micro-sized parts as it is considered such an important factor but is not of high concern during conventional injection moulding. De Santis *et al*. [7] developed a system whereby the mould surface temperature could be increased by some tenths of a Celsius degrees in a matter of a second. This technology boasted results of double part length with the same input energy when using a semi-crystalline polymer. Vacuum venting is another type of technology that can be applied to µIM to improve part outcome and thus reduce energy costs. Ying Choi *et al*. [8] have shown that by vacuum venting during the injection phase of the µIM process can create more defined features over larger areas and increased depths. Depth replication was improved by 1.33-7.52% and 0.88-5.94% by varying the vacuum pressure and time respectively. Thus showing that the vacuum pressure plays more of role with regards to µIM.

A material studied in research to be used as a coating has been Diamond-like carbon (DLC). DLC coatings belonged to the amorphous hydrogenated carbon (aC:H) group with diamond-like properties of high hardness, low coefficient of friction as well as a high wear resistance makes it an

*College of Engineering, Swansea University, Swansea SA1 8EN, UK;
Tel: +44(0)1792295514; E-mail: c.a.griffiths@swansea.ac.uk

attractive choice for many engineering sectors [9]. aC:H coatings have previously been utilised in applications such as magnetic storage devices, coatings for manufacturing tools, razor blades, watches, automotive parts, micro-electromechanical devices, semiconductors and microactuators [10]. Surgical implants have also been explored and aC:H coatings on the industry standard Nickel Titanium (Ni-Ti), have shown to improve endothelialisation compared to non-coated implants. Adhesion, morphology, and viability of endothelial cells on implants with aC:H coatings were improved. It has also been shown that except for 0-0.22 μm wear debris (WD), cytotoxicity levels are decreased with aC:H coated artificial joints [11]. Another major benefit of coatings is that they exhibit increased antimicrobial properties compared to normal steels [12]; enhancing this coating for medical μIM applications.

Even though aC:H coatings have been shown to improve the lifetime of micro-moulds during their use in industrial processes, there has also been evidence that wear and delamination can occur during continued processing [13]. In particular, there is the need to understand how well aC:H coatings can withstand failure so that recommendations can be made to industrial users as to how to prevent them under specific conditions. One such condition is the thermal expansion behaviour that a mould and its coating can experience during temperature variations of a process such as μIM. Having a large difference in the thermal expansion coefficient of the substrate of the mould and its coating, high stress can be generated within the coating leading to delamination, cracking or even complete failure [14].

The research presented in this paper follows on from Griffiths *et al*. [15]; where previous work where Finite Element Analysis (FEA) simulation was carried out on a micro-mould to identify areas of the tool surface that experiences sudden heat variation. The same substrate was used with the deposition of a aC:H coating on a Stainless Steel (SS) micro-mould in order to investigate how the coating withstood thermal cycling. To measure this, the length and width of 5 micro-cracks were studied with theoretical predictions and verified with experimental data.

The next section of this research journal reviews surface treatment technologies used in μIM along with their functionalities and how their applications are justified. In the following section, the theory of thermal expansion is explained. Finally, the experimental setup is detailed in the last sections showing the results of the research along with conclusions.

2. TOOLING SURFACE TECHNOLOGIES

Advanced powder metallurgy tool steels with a high content of hard carbide particles to cast martensitic matrix steels were the point of call for improving the wear resistance of moulding surfaces [16]. In more recent years, coating technologies, along with functional coating surfaces, have been implemented to improve wear resistance for many engineering surfaces [17-20]. In extreme engineering environments, like desalination plants, it has been shown that coatings with functional properties, like aC:H, can be added to SS to decrease the corrosion rates [21]. Functional coatings can be developed through processes such as innovative grinding systems, sandblasting, focus ion beam, chemical texturing, laser machining and nano-imprint lithography [18, 19, 22, 23].

2.1. Coated Surfaces

aC:H coatings are most commonly used for coatings of plastic injection moulding inserts [24]. The coatings have been proven to improve the repeatability of the micro and nano-structured master inserts [17]. The reasoning for this is down to a combination of superior tribological and mechanical properties such as low friction, low wear, and high hardness, whereas traditional tool materials lack these properties [13, 25, 26].

As mentioned previously, aC:H has a low friction coefficient and in μIM, the surface roughness is a major factor for thin cavities and Bellantone *et al*. [27] have found that this is emphasised as the moulding scale is decreased. With decreasing cavity depths, higher surface roughness promotes the filling phase as it allows the melt to flow forward into the cavity. This phenomenon is explained to be as a result of both the high shear effect and the reduced the polymer viscosity.

This results in low wear surface characteristic and it can be explained by the high ratio between the hardness, Young's modulus and the low ratio between the surface energy and hardness [9]. The usual practice is that the surface treatment of inserts is performed using pulsed laser deposition (PLD) of coatings which yields surface hardness of up to 70 GPa with friction coefficients in the range of 0.05–0.2. Ceramic coatings exhibit surface hardness and coefficient of friction levels much greater than these levels [28]. Super low friction coefficients of 0.003–0.008 were achieved by Heimberg *et al*. [29] by paying particular attention to the gas-surface interactions and duty cycles with control variables of time and speed. The effect of surface properties of microstructured master inserts on the hot embossing process has been investigated by Saha *et al*. [30] using nitrogen (N) and nickel (Ni) doped with diamond-like carbon (N:DLC:Ni) coated and uncoated silicon (Si) micro moulds. Even with high friction and adhesion properties, the results showed that the N:DLC:Ni coated Si master inserts increased the mould longevity by 3-18 times in comparison to uncoated moulds.

aC:H film preparation can also be completed by Plasma Enhanced Chemical Vapour Deposition (PECVD). However, varying Argon (Ar) and Hydrogen (H) can give a wide range of results. Toro *et al*. [31] reported that with varying H flow during the deposition, aC:H tends to resist depositing in aggressive environments while delamination of the coating

was held accountable by varying Ar rates. Sasaki *et al.* [32] studied the ejection force (F_e) but varied the tool surface roughness and the tool surface coatings for the investigation. The experimental results demonstrated that when moulding Polypropylene (PP) and Polyethylene terephthalate (PET), F_e and product deformation were reduced when the surface roughness of the inserts was in the range of R_a from 0.212 to 0.026. The Poly(methyl methacrylate) (PMMA) samples did not require such a high F_e when surface roughness was R_a of 0.092. Also, the results showed that any F_e reductions were dependent both on the optimised surface roughness and the polymer material used in the moulding trials. Another conclusion from this investigation was that the PVD WC/C carbon coating was the most effective in reducing F_e [32].

The tribological behaviour of aC:H coated 100C6-steel substrate when subjected to a temperature increase from room temperature to 400 °C has been investigated by Bremond *et al.* [33]. The aC:H being used in this investigation belonged to the amorphous hydrogenated carbon coatings' group. When the coated steel substrate increased above 200 °C, the coating damage increases dramatically due to stiffness reduction of the 100C6 steel.

In µIM, large surface area to volume ratios are normal and this results in high adhesion forces between the mould and the tool surface [30]. However, Griffiths *et al.* [17] reported that if the mould surface is coated with aC:H when moulding Polycarbonate (PC) and Acrylonitrile butadiene styrene (ABS) polymers, a F_e reduction of 40% and 16% were achieved, respectively, in comparison with untreated surfaces. Using aC:H coatings in microreplication processes has proven to yield solid outcomes [30].

2.2. The Possible Causes of Coating Delamination

Prediction ability of interfacial delamination of coatings has major advantages to accurate lifetime assessment of products under working conditions. Di Leo *et al.* [34] investigated the delamination properties of thermal barrier coatings (TBC) carrying out simulations in order to predict the relevant material parameters appearing in a traction-separation-type law. TBC system parameters are now determined using the data revealed in this study. Kang *et al.* [35] studied the delamination of aC:H films on titanium alloys. By depositing a TiCN interlayer between the Ti-6Al-4V alloy and the aC:H film, it was concluded that an improvement in hardness, Young's modulus and interfacial bonding can be achieved. To add to this, the resulting coefficient of friction was 0.03. Escudeiro *et al.* [36] studied the wear properties of Ultra-high-molecular-weight polyethylene (UHMWPE) and Polyether ether ketone (PEEK) when in contact with DLC and Zr-DLC coatings. During this investigation, each material was subjected to 2 million cycles (Mc). Zr-DLC was found to delaminate after 1.2 Mc. Synergetic stress-induced corrosion caused the delamination which introduces interface fatigue.

The application of aC:H on enhancing the longevity of the artificial joint was investigated by Zhang *et al.* [37]. Different substrate materials such as SS, CoCrMo and titanium alloys were used in this investigation. It was found that the failure mode of DLC coatings on 316 SS and CoCrMo alloy through friction testing was coating delamination. Another conclusion to this study was that aC:H coating on Ti-6Al-4V has superior wear resistance: presenting better stability in immersion and electrochemical tests as added advantage.

DLC has previously been attributed to limited tribological applications where the requirements are high contact stresses leading from high residual stresses [38]. To counteract this, Lin *et al.* [39] have investigated the feasibility of using an alternate soft and hard layer of aC:H on M2 steel substrates. A multilayer coating with a soft top layer of aC:H had increased wear resistance compared to that of a standard single layer coating. Also, with increasing percentage of hard layer thickness, the residual stress, hardness and reduced modulus are increased.

Two-step heat treatment on hardness, fracture toughness and wear has been investigated by Zia *et al.* [40]. For aC:H coatings deposited without a buffer layer on silicon substrates. They reported that one step heat treatment of 300°C for 30mins with a 20 hour cool time decreases hardness and fracture toughness by up to 20%. While two-step heat treatments, 150°C for 30mins with a 20 hour cool time which is then repeated, retained original values along with an increase of 43% and 9% for hardness and fracture toughness respectively, for certain deposition configurations.

3. THERMAL EXPANSION

Cyclical temperature gradients in µIM are of a result of mechanical interactions such as shear stress, injection pressure, clamping force and friction between the resulting mould surface and polymer melt. The processing stages of filling (heating) and cooling during µIM, also affect the temperature gradient. During the transient change of temperature and the thermal expansion variation between the tool and the coating substrate, delamination of the coatings is very likely to occur.

3.1. Linear Thermal Expansion

The average coefficient of linear thermal expansion ($\propto_{t_2-t_1}$) is an expression for the change in length of a solid body during a variation in temperature. This is dependent on the original length and the temperature change of heating and cooling. It is defined in Eq. (1) as:

$$\propto_{t_2}^{t_1} = \frac{L_2 - L_1}{L_R(t_2 - t_1)} \tag{1}$$

where (t_1) and (t_2) are the initial and final temperatures, (L_1) and (L_2) are the initial and final lengths, respectively, and (L_R) is the length at a reference temperature.

The instantaneous coefficient of linear expansion at any temperature, (t), can be defined by the equation Eq. (2) as:

$$\propto_t = \lim_{t_1 \to t_2}\left(\frac{L_2 - L_1}{L_R(t_2 - t_1)}\right) = \frac{dL}{L_R(dt)} \qquad (2)$$

where (α_t) is the instantaneous coefficient of linear expansion at a given temperature (t).

Therefore, the fractional change in length (ΔL) of a solid subjected to linear thermal expansion is given by Eq. (3) as:

$$\frac{\Delta L}{L_0} = \alpha \Delta T \qquad (3)$$

where (α) is the coefficient of thermal expansion, (L_0) is the initial length and (ΔT) is the change of temperature to which the material is subjected.

3.2. Superficial Thermal Expansion

In Section 3.1, thermal expansion of the tooling during processing has been proven. This will influence the resulting tooling dimensions which will be subjected to superficial thermal expansion. Utilising the terms of Eq. (3), the calculation can be further expanded to incorporate the new superficial change in length (L) which can be seen incorporated in Eq. (4) below which is the final length (L). This is known by defining a new representation of a new superficial length (L) using the terms of equation Eq. (3) and since L=L_0+ΔL is known, then finally:

$$L = L_0 + L_0\alpha T = L_0(1 + \alpha\Delta T) \qquad (4)$$

A micro rib feature of a rectangular surface with an area (A_0); can be obtained by the product of its height (H_0) and its width (W_0). The effect of the temperature in both (H_0) and (W_0) result in the new area defined by the following equation:

$$A = HW = H_0(1+\alpha\Delta T)W_0(1+\alpha\Delta T) = H_0W_0(1+\alpha\Delta T)(1+\alpha\Delta T)$$
$$A = A_0[1 + 2\alpha\Delta T + (\alpha\Delta T)^2] \qquad (5)$$

The value of (α) is typically small and for small temperature change, (αΔT) is significantly lesser than 1. This allows for concluding that the term $(\alpha\Delta T)^2$ in the previous equation is basically negligible compared to the (2αΔT) term. Thus,

cancelling this expression, the following equation defines the new area of an object subjected to thermal expansion, which is given by:

$$A = A_0(1 + 2\alpha\Delta T) \qquad (6)$$

With film-substrates being used for a wide range of applications, investigations into this behaviour with respect to the mechanical aspects along with the thermodynamics are critical. During the cycle time of μIM, high temperature hysteresis profiles are present due to cyclic heating, cooling and localised shear stress. Variation of the polymer temperature when processing can also cause variations to the mould longevity. Lastly, with the inherent volumetric change during the processing of polymers through μIM, interactions occur between processing variables such as injection pressure, shear stress, clamping force and friction between the resulting mould surface and polymer melt. As mentioned, this study follows on from the previous investigation analysing the difference in thermal expansion between the polymer melt and aC:H coated SS substrate [15]. Here, micro-indentations are purposely imposed upon the substrate to conclude the feasibility of DLC coatings within μIM.

4. EXPERIMENTAL SET-UP

4.1. Part and Mould Design

The substrate used in this paper was a micro-replication mould made from SS304 with outer dimensions 28 mm x 25 mm x 5 mm (Figure **1b**). The replicated microfluidic part, created via μIM, has dimensions of 15 x 22 x 1 mm (Figure **1a**). The microstructures of the replicated part have dimensions up to 100 μm.

4.2. aC:H Surface Treatment

In order to improve the coating adhesion of the substrate, two layers were added to the original SS mould. Firstly, a 0.5 μm silicon carbide intermediate layer and then a 2 μm layer of aC:H film was deposited at 320 W/625 V with a working pressure of 4Pa along with 20% of H_2 in (C_6H_{12} + H_2) mixture using a Plasma Assisted Chemical Vapour Deposition (PACVD) machine. Table **1** provides the surface properties.
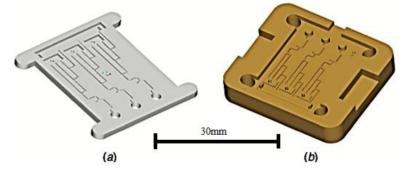

30mm

(a)　　　(b)

Figure 1: A graphical representation of the SS microreplication mould (**b**) and its replicated microfluidic part (**a**) created via μIM.

Table 1:   Properties of the aC:H Layer Produced on the SS Micro-Mould using a PACVD Machine

Properties	Typical Value
Coating Thickness (μm)	2.5
Micro-hardness (GPa)	22 ± 2
Coefficient of Friction	0.05
Young Modulus (GPa)	160 ± 10
Wear Rate $(mm^3\, N^{-1}\, m^{-1})$	5×10^{-7}

4.3. Micro Indentation

Damage marks on the aC:H coating of the substrate were required in order to analyse the fracture behaviour during thermal cycling. These intentional marks were created by indenting the coating using a Buehler Micromet 5114 micro-indentation hardness testing machine with a sphere-conical diamond 120º cone with a 0.2 mm tip radius under a load of 1000 gf for 10 seconds. Several cracks were selected in order to study crack growths and propagations as well as the increase in the size of delaminated zones after thermal cycles. These experiments allowed this study to get the conclusions that summarise the temperature effects on a coated tool. Figures **2** and **3** illustrate a total of eleven micro-indentation marks that were performed in this study in different parts of the micro-mould. The morphology and geometry, specifically the length, width, depth and surface roughness of the cracks after each thermal cycle were analysed using a HITACHI Scanning Electron Microscope (SEM) S-3400N and an OLYMPUS LEXT OLS4000 confocal microscope. It was found that the micro-indentation marks created a number of coating cracks and chipped zones (Figures **4** and **5**). Five observable cracks and major chip delamination caused by the micro-indentation process were chosen in order to conduct a further analysis that will look crack growth and/or propagation along with delamination of the chip caused by temperature changes of the mould.

4.4. Metrology

Figure **6** shows how the length and width of the cracks chosen for analysis were measured using both the confocal microscope and SEM. Table **2** displays the data obtained from each of the cracks chosen from each indentation mark.
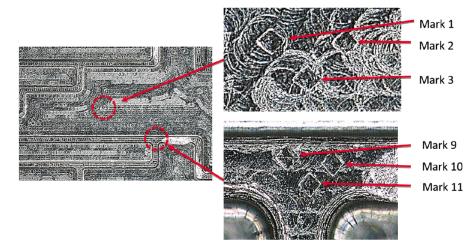

Figure 2: Identification of the micro-indentation marks 1 to 3 and 9 to 10 on the workpiece at 20 x magnification.
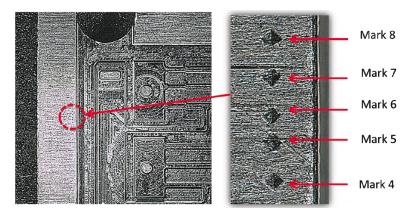

Figure 3: Identification of the micro-indentation marks 4 to 8 on the workpiece at 20 x magnification.
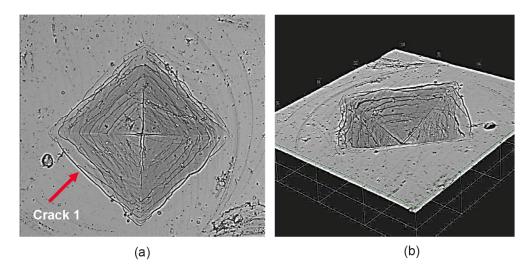
Figure 4: (**a**) Crack 1 selected from indentation mark 1 (**b**) 3D picture of indentation mark 1, both at 100x magnification.
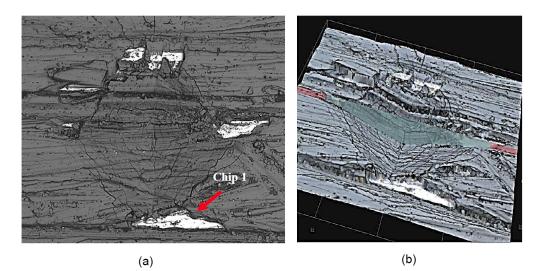

Figure 5: (**a**) Delaminated chip 1 selected from indentation mark 5 and (**b**) 3D picture of indentation mark 5, both at 100x magnification.
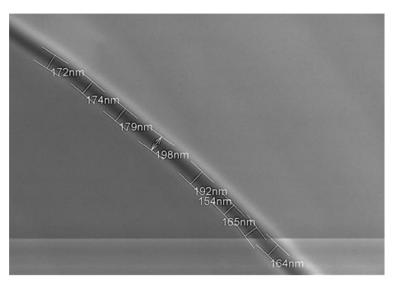

Figure 6: Crack width measurements using a SEM at 20 kV and 30.000x magnification.

Table 2: **The Length and Average Width Measurements for each Crack Identified in the Indentation Marks Created in the aC:H Layer, as well as the Height of the Corresponding Marks**

Micro-indentation marks		Crack/Chip Data		
No.	Height (µm)	No.	Length (µm)	Average Width (nm) Sample size: 10 Measurments
1	13.79	1	42.74	127.10
2	12.84	2	55.54	150.30
3	13.31	3	47.98	232.00
4	12.25	4	32.64	212.80
5	12.24	1	11.12	45.85

4.5. Temperature Cycle

To analyse the behaviour of the cracks under repetitive thermal stresses, the coated micro-mould was heated in a Carbolite 213 oven to a temperature of 265 ºC for one hour and then left to cool for a period of two hours. This thermal cycle was repeated ten times with a final thermal cycle fixed to the same temperature but held for eight hours as opposed to the original one hour holding time. The following steps were followed in this experiment:

1. The micro-mould was heated-up in an oven at a temperature of 265 ºC, simulating the injection temperature of ABS, for a time of one hour.

2. After the thermal cycle, the tool was left to cool to room temperature under no special cooling techniques for a time of two hours.

3. A SEM was then used to measure the crack widths selected and a confocal microscope was employed to obtain the crack lengths.

5. The heating cycle described in step 1 to 2 was repeated nine more times.

6. The micro-mould was subjected to an eleventh heat treatment where it was heated-up at 265 ºC for a time of eight hours.

7. The measurements in step 3 were repeated.

8. Finally, the workpiece was cleaned in an ultrasonic tank for fifteen minutes at 55 ºC and 40kHz using 29 litres of water mixed with 100 ml of cleaning detergent (Ultraclean M Formula II) and 100 mg of sodium hydroxide.

9. The final crack dimensional measurements were then taken.

5. RESULTS & DISCUSSION

5.1. Thermal Linear Expansion

During the thermal cycles induced during injection moulding, thermal expansion of both the SS mould and the coating can occur resulting in residual stresses being induced in the substrate. Theoretically, the fractional change in length resulting from this thermal expansion can be calculated using Eq. (3). This was used to predict the dimensional growth of the cracks identified. These predicted lengths and widths are presented in Table **3**, calculated using the parameters as follows: a 2.5 µm thick layer of coating, starting temperature of 20 ºC and a thermal expansion coefficient of 2.3×10^{-6} ºC^{-1} for a temperature of 265 ºC. As can be seen from these values, it is expected that the cracks within each chip will grow under a temperature increase and result in a change in length (ΔL) (Figure **7**).

5.2. Surface Cracking Variation after Thermal Cycles

To validate the theoretical predictions, the average of eight experimental measurements for each identified crack width and length are presented in Figure **8** for width and Figure **9**

Table 3: **The original length and width of the cracks identified in each indentation mark prior to any temperature change, and the predicted growth in these values after heating from 20 ºC to 265 ºC: these use the equations (1), (2) and (3) in order to make averaged predictions for the Preheat (PH) process**

Mark No.	Crack/Chip No.	Preheating (PH)		Theoretical	
		Length (µm)	Average Width (nm)	Length (µm)	Average Width (nm)
1	1	42.74	127.10	42.76	127.17
2	2	55.54	150.30	55.57	150.38
3	3	47.98	232.00	48.01	232.13
4	4	32.64	212.80	32.66	212.92
5	1	11.12	45.85	11.13	45.88

for length. In both figures, PH measurements, the measurements over ten thermal cycles, the measurements after the extended (LONG) heat treatment and measurements taken after final ultrasonic cleaning (US) are shown.
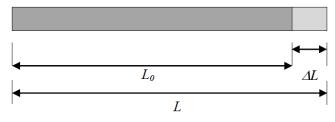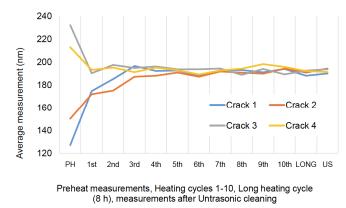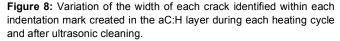

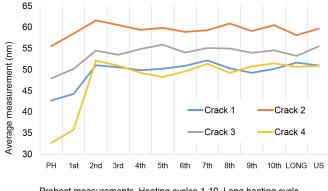**Figure 7:** Thermal linear expansion effect of solids.

Cracks 1 and 2 displayed an increase in width of 37% and 15%, respectively, during the first thermal cycle. As mentioned, a difference in the coefficients of expansion between the SS substrate and the aC:H coating will result in stresses within the coating layer allowing the cracks to expand during the temperature change. Also, a variation in the material microstructure; a change in the size of the grains within both materials may be changing from a fine to a coarse grain. This may also be exacerbated by the growth of oxide layers during the heat treatment leading to a larger volume difference between the aC:H coating and the SS.

Alternatively, cracks 3 and 4 display a decrease in width by 18% and 10% respectively. A common factor for the cracks measured is that their widths level after the third heat cycle is within a range of 190 to 195 nm. This can be explained by considering that the aC:H coating reaches plastic deformation yield point of 265 ºC, meaning that some deformations in the material become irreversible; resulting in stabilisation of the crack widths.

Unlike the crack widths, the length of each crack increases during the thermal cycles. In particular, after the second heat treatment, the cracks increase in length by 20%, 10%, 15% and 60% respectively. Similarly, to the width, the lengths of the cracks level after the second heat treatment, show no more growth during the subsequent heat cycles.
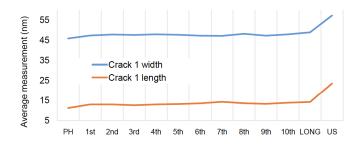

Preheat measurements, Heating cycles 1-10, Long heating cycle (8 h), measurements after Untrasonic cleaning

Figure 8: Variation of the width of each crack identified within each indentation mark created in the aC:H layer during each heating cycle and after ultrasonic cleaning.

Preheat measurements, Heating cycles 1-10, Long heating cycle (8 h), measurements after Untrasonic cleaning

Figure 9: Variation of the length of each crack identified within each indentation mark created in the aC:H layer during each heating cycle and after ultrasonic cleaning.

5.3. Chip Delamination

The chips from which the cracks were identified were also measured before and after the thermal cycles. The results in Figure **10** show that after the first thermal cycle, the chip grew from 45.85 nm to 47.31 nm in width and 11.12 nm to 12.9 nm in length. After this cycle, the chip did not display any change in dimensions until the ultrasonic cleaning had been applied. The ultrasonic cleaning resulted in an increase in width of 17% and an increase in length of 65%. This growth suggests

Preheat measurements, Heating cycles 1-10, Long heating cycle (8 h), measurements after Untrasonic cleaning

Figure 10: Variation in the width and length of the mark identified as Chip 1 during each heating cycle and after ultrasonic cleaning.
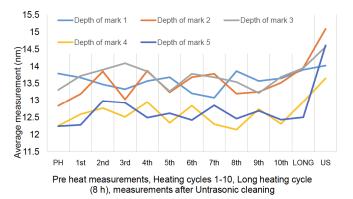

Pre heat measurements, Heating cycles 1-10, Long heating cycle (8 h), measurements after Untrasonic cleaning

Figure 11: Behaviour of the height of indentation marks on a aC:H coated micro-tool after thermal cycles.

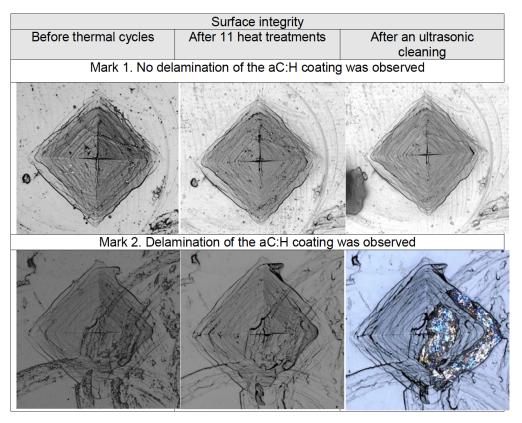| Surface integrity		
Before thermal cycles	After 11 heat treatments	After an ultrasonic cleaning
Mark 1. No delamination of the aC:H coating was observed		
Mark 2. Delamination of the aC:H coating was observed		

Figure 12: Delamination of the aC:H before and after the heat cycles and the ultrasonic cleaning.

that the thermal cycles weakened the bond between the aC:H coating and the SS substrate within the chip and the surrounding areas: resulting in delamination when the ultrasonic cleaning was carried out. This also affected the depth of each chip. Figure **11** shows that chip 2, 4 and 5 experienced an increase in depth of 17%, 11% and 20% respectively. This delamination result can also be seen in the SEM images of each chip taken before the thermal cycles, after, and after the ultrasonic cleaning process: as shown in Figure **12**.

5.4. Surface Inspection of Areas Without Wear or Damage

The above analysis concludes the effect of thermal cycling on the integrity of damaged aC:H coating on a SS substrate. The results suggest that thermal cycling affects the adherence of the coating when there is wear or damage present. However, it was also concluded, by analysing the surface roughness (R_a and R_z) of the tool wear and damage free zones (Figures **13** and **14**), that the thermal cycles do not negatively affect the surface of the coating on the SS substrate. In addition to surface roughness, the mould area was briefly analysed using the SEM to see if there was any damage. The results showed that there was no degradation in the areas that were unaffected by deliberate damage, suggesting that the stresses introduced in the surface through the thermal coefficient of expansion difference does not negatively affect the bonding of the coating to the tool surface during thermal cycling.
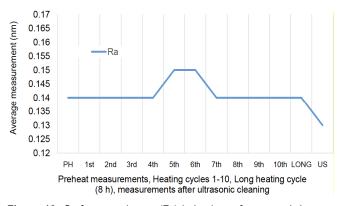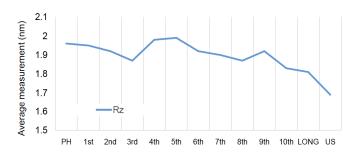

Preheat measurements, Heating cycles 1-10, Long heating cycle (8 h), measurements after ultrasonic cleaning

Figure 13: Surface roughness (R_a) behaviour of wear and damage free DLC coating after heat treatments.

Preheat measurements, Heating cycles 1-10, Long heating cycle (8 h), measurements after ultrasonic cleaning

Figure 14: Surface roughness (R_z) behaviour of wear-free DLC coating after thermal cycling.

6. CONCLUSIONS

The aim of this research was to determine the effect of thermal cycles on the integrity of damaged aC:H coating on a SS microreplication mould being used for µIM purposes. To study the coating under normal wear and tear conditions, several damaged areas were created on the coating surface by using a micro-indentation hardness testing machine. Cracks were identified within these damaged areas and their length and width propagation were followed over 10 heating cycles, a long heating cycle and after ultrasonic cleaning.

- It was concluded that cracks will propagate and grow under thermal cycle conditions due to the stresses induced by thermal expansion of the coating. Theoretical analyses of the micro-cracks were predicted before experimental analysis with very close comparisons being presented. The first and second heat cycles had the most significance to the growth of the cracks: with a near plateau therefore after. The reasoning for this is the difference in the coefficients of thermal expansion between the SS and the aC:H coating which leads to stresses within the aC:H allowing the cracks to expand during the temperature variations.

- It was observed that the damage free areas of the aC:H coating do not suffer negatively under thermal expansion effects agreeing with the claim that aC:H coatings behave well for mould tool applications. The R_a and R_z did not change significantly during the testing and in fact, the surface roughness decreased 0.01 nm and 0.27 nm respectively.

- The final conclusion made was that after the surface damage the effects of thermal expansion can weaken the adhesion of the aC:H coating to the substrate material: resulting in delamination effects particularly during the ultrasonic cleaning process. Chip 1 exhibited an increase in width of 17% and an increase in length of 65% after ultrasonic cleaning. By identifying the areas of high stress and areas of potential surface damage it is possible to control the cavity filling process in order to preserve the tool from damage.

- This research showed that the positive effects of aC:H coatings can be maintained under the thermal cycles induced during the injection moulding process, so long as there is no inherent damage present on the surface of the coating. Some areas and features of the tool: such as micro ribs with a high surface to volume ratio may be susceptible to damage, especially during part demoulding.

ACKNOWLEDGEMENTS

REFERENCES

[1] Tosello G, Hansen HN. Chapter 6 - Micro-Injection-Molding A2 - Qin, Yi, Micro-Manufacturing Engineering and Technology, William Andrew Publishing, Boston, 2010; pp. 90-113. (ISSN 978-0-8155-1545-6).

[2] Piotter V, Mueller K, Plewa K, Ruprecht R, Hausselt J. Performance and simulation of thermoplastic micro injection molding. Microsystem Technologies 2002; 8: 387-390.
http://dx.doi.org/10.1007/s00542-002-0178-6

[3] Navabpour P, Teer DG, Hitt DJ, Gilbert M. Evaluation of non-stick properties of magnetron-sputtered coatings for moulds used for the processing of polymers. Surface and Coatings Technology 2006; 201: 3802-3809.
http://dx.doi.org/10.1016/j.surfcoat.2006.06.042

[4] Masato D, Sorgato M, Parenti P, Annoni M, Lucchetta G. Impact of deep cores surface topography generated by micro milling on the demolding force in micro injection molding. Journal of Materials Processing Technology 2017; 246: 211-223.
http://dx.doi.org/10.1016/j.jmatprotec.2017.03.028

[5] Menges G, Mohren P. How to Make Injection Molds, Hanser Publishers1993; (ISSN 9780195210088).

[6] Griffiths CA, Dimov SS, Scholz SG, Tosello G, Rees A. Influence of Injection and Cavity Pressure on the Demoulding Force in Micro-Injection Moulding. Journal of Manufacturing Science and Engineering 2014; 136: 031014-031014-031010.
http://dx.doi.org/10.1115/1.4026983

[7] De Santis F, Pantani R. Development of a rapid surface temperature variation system and application to micro-injection molding. Journal of Materials Processing Technology 2016; 237: 1-11.
http://dx.doi.org/10.1016/j.jmatprotec.2016.05.023

[8] Ying Choi S, Zhang N, Toner JP, Dunne G, Gilchrist MD. Vacuum Venting Enhances the Replication of Nano/Microfeatures in Micro-Injection Molding Process. Journal of Micro and Nano-Manufacturing 2016; 4: 021005-021005-021007.
http://dx.doi.org/10.1115/1.4032891

[9] Robertson J. Properties of diamond-like carbon. Surface and Coatings Technology 1992; 50: 185-203.
http://dx.doi.org/10.1016/0257-8972(92)90001-Q

[10] Sasaki S, Yagi T, Mano H, Miyake K, Nakano M, Ishida T. Effect of Tribochemical Reaction on Friction and Wear of DLC under Lubrication with Ionic Liquids at High-Vacuum Condition, in: J. Luo, Y. Meng, T. Shao, Q. Zhao (Eds.) Advanced Tribology: Proceedings of CIST2008 & ITS-IFToMM2008, Springer Berlin Heidelberg, Berlin, Heidelberg, 2010; pp. 886-887. (ISSN 978-3-642-03653-8).

[11] Liao TT, Deng QY, Li SS, Li X, Ji L, Wang Q, Leng YX, Huang N. Evaluation of the Size-Dependent Cytotoxicity of DLC (Diamondlike Carbon) Wear Debris in Arthroplasty Applications. ACS Biomaterials Science & Engineering 2017.
http://dx.doi.org/10.1021/acsbiomaterials.6b00618

[12] Robertson SN, Gibson D, MacKay WG, Reid S, Williams C, Birney R. Investigation of the antimicrobial properties of modified multilayer diamond-like carbon coatings on 316 stainless steel. Surface and Coatings Technology 2017; 314: 72-78.
http://dx.doi.org/10.1016/j.surfcoat.2016.11.035

[13] Saha B, Liu E, Tor SB, Hardt DE, Chun JH, Khun NW. Improvement in lifetime and replication quality of Si micromold using N:DLC:Ni coatings for microfluidic devices. Sensors and Actuators B: Chemical 2010; 150: 174-182.
http://dx.doi.org/10.1016/j.snb.2010.07.019

[14] Arsenault RJ, Shi N. Dislocation generation due to differences between the coefficients of thermal expansion. Materials Science and Engineering 1986; 81: 175-187.
http://dx.doi.org/10.1016/0025-5416(86)90261-2

[15] Griffiths CA, Rees A, Kerton RM, Fonseca OV. Temperature effects on DLC coated micro moulds. Surface and Coatings Technology 2016; 307(Part A): 28-37.
http://dx.doi.org/10.1016/j.surfcoat.2016.08.034

[16] Jeglitsch F. Tool Steels in the Next Century: Proceedings of the 5th International Conference on Tooling, September 29th to October 1st 1999, University of Leoben, Leoben, Austria, Institut fur Metallkunde und Werkstoffprufung, Montanuniversitat Leoben1999; (ISSN 9783950110500).

[17] Griffiths CA, Dimov SS, Brousseau EB, Chouquet C, Gavillet J, Bigot S. Investigation of surface treatment effects in micro-injection-moulding. The International Journal of Advanced Manufacturing Technology 2010; 47: 99-110.
http://dx.doi.org/10.1007/s00170-009-2000-4

[18] Martínez E, Engel E, Planell JA, Samitier J. Effects of artificial micro- and nano-structured surfaces on cell behaviour. Annals of Anatomy - Anatomischer Anzeiger 2009; 191: 126-135.
http://dx.doi.org/10.1016/j.aanat.2008.05.006

[19] Kovalchenko A, Ajayi O, Erdemir A, Fenske G, Etsion I. The effect of laser surface texturing on transitions in lubrication regimes during unidirectional sliding contact. Tribology International 2005; 38: 219-225.
http://dx.doi.org/10.1016/j.triboint.2004.08.004

[20] Dimitrov AS, Nagayama K. Continuous Convective Assembling of Fine Particles into Two-Dimensional Arrays on Solid Surfaces. Langmuir 1996; 12.
http://dx.doi.org/10.1021/la9502251

[21] Golsefatan HR, Fazeli M, Mehrabadi AR, Ghomi H. Enhancement of corrosion resistance in thermal desalination plants by diamond like carbon coating. Desalination 2017; 409: 183-188.
http://dx.doi.org/10.1016/j.desal.2017.01.027

[22] Bruzzone AAG, Costa HL, Lonardo PM, Lucca DA. Advances in engineered surfaces for functional performance. CIRP Annals - Manufacturing Technology 2008; 57: 750-769.
http://dx.doi.org/10.1016/j.cirp.2008.09.003

[23] Chou SY, Krauss PR, Renstrom PJ. Imprint of sub-25 nm vias and trenches in polymers. Applied Physics Letters 1995; 67: 3114-3116.
http://aip.scitation.org/doi/abs/10.1063/1.114851

[24] Griffiths CA, Dimov SS, Rees A, Dellea O, Gavillet J, Lacan F, Hirshy H. A novel texturing of micro injection moulding tools by applying an amorphous hydrogenated carbon coating. Surface and Coatings Technology 2013; 235: 1-9.
http://dx.doi.org/10.1016/j.surfcoat.2013.07.006

[25] Tillmann W, Vogli E, Hoffmann F. Wear-resistant and low-friction diamond-like-carbon (DLC)-layers for industrial tribological applications under humid conditions. Surface and Coatings Technology 2009; 204: 1040-1045.
http://dx.doi.org/10.1016/j.surfcoat.2009.06.005

[26] Voevodin AA, Rebholz C, Matthews A. Comparative Tribology Studies of Hard Ceramic and Composite Metal-DLC Coatings in Sliding Friction Conditions. Tribology Transactions 1995; 38: 829-836.
http://dx.doi.org/10.1080/10402009508983476

[27] Bellantone V, Surace R, Modica F, Fassi I. Effect of Surface Roughness in Micro Injection Moulding Process of Thin Cavities 2016.
http://dx.doi.org/10.1115/DETC2016-59968

[28] Voevodin AA, Donley MS, Zabinski JS. Pulsed laser deposition of diamond-like carbon wear protective coatings: a review. Surface and Coatings Technology 1997; 92: 42-49.
http://dx.doi.org/10.1016/S0257-8972(97)00007-8

[29] Heimberg JA, Wahl KJ, Singer IL, Erdemir A. Superlow friction behavior of diamond-like carbon coatings: Time and speed effects. Applied Physics Letters 2001; 78: 2449-2451.
http://aip.scitation.org/doi/abs/10.1063/1.1366649

[30] Saha B, Liu E, Tor SB, Khun NW, Hardt DE, Chun JH. Replication performance of Si-N-DLC-coated Si micro-molds in micro-hot-embossing. Journal of Micromechanics and Microengineering 2010; 20: 045007.
http://stacks.iop.org/0960-1317/20/i=4/a=045007

[31] Toro RG, Calandra P, Cortese B, de Caro T, Brucale M, Mezzi A, Federici F, Caschera D. Argon and hydrogen plasma influence on the protective properties of diamond-like carbon films as barrier coating. Surfaces and Interfaces 2017; 6: 60-71.
http://dx.doi.org/10.1016/j.surfin.2016.11.009

[32] Sasaki T, Koga N, Shirai K, Kobayashi Y, Toyoshima A. An experimental study on ejection forces of injection molding. Precision Engineering 2000; 24: 270-273.
http://dx.doi.org/10.1016/S0141-6359(99)00039-2

[33] Bremond F, Fournier P, Platon F. Test temperature effect on the tribological behavior of DLC-coated 100C6-steel couples in dry friction. Wear 2003; 254: 774-783.
http://dx.doi.org/10.1016/S0043-1648(03)00263-1

[34] Di Leo CV, Luk-Cyr J, Liu H, Loeffel K, Al-Athel K, Anand L. A new methodology for characterizing traction-separation relations for interfacial delamination of thermal barrier coatings. Acta Materialia 2014; 71: 306-318.
http://dx.doi.org/10.1016/j.actamat.2014.02.034

[35] Kang S, Lim H-P, Lee K. Effects of TiCN interlayer on bonding characteristics and mechanical properties of DLC-coated Ti-6Al-4V ELI alloy. International Journal of Refractory Metals and Hard Materials 2015; 53(Part A): 13-16.
http://dx.doi.org/10.1016/j.ijrmhm.2015.04.028

[36] Escudeiro A, Wimmer MA, Polcar T, Cavaleiro A. Tribological behavior of uncoated and DLC-coated CoCr and Ti-alloys in contact with UHMWPE and PEEK counterbodies. Tribology International 2015; 89: 97-104.
http://dx.doi.org/10.1016/j.triboint.2015.02.002

[37] Zhang HL, Ong NS, Lam YC. Experimental investigation of key parameters on the effects of cavity surface roughness in microinjection molding. Polymer Engineering & Science 2008; 48: 490-495.
http://dx.doi.org/10.1002/pen.20981

[38] Voevodin AA, Walck SD, Zabinski JS. Architecture of multilayer nanocomposite coatings with super-hard diamond-like carbon layers for wear protection at high contact loads. Wear 1997; 203: 516-527.
http://dx.doi.org/10.1016/S0043-1648(96)07425-X

[39] Lin Y, Zia AW, Zhou Z, Shum PW, Li KY. Development of diamond-like carbon (DLC) coatings with alternate soft and hard multilayer architecture for enhancing wear performance at high contact stress. Surface and Coatings Technology 2017; 320: 7-12.
http://doi.org/10.1016/j.surfcoat.2017.03.007

[40] Zia AW, Zhou Z, Shum PW, Li LKY. The effect of two-step heat treatment on hardness, fracture toughness, and wear of different biased diamond-like carbon coatings. Surface and Coatings Technology 2017; 320: 118-125.
http://dx.doi.org/10.1016/j.surfcoat.2017.01.089